Jurnal Teknologi

Full Paper

Hibiscus sabdariffa Linn. WATER-ETHANOL EXTRACT NANOEMULSION FOR RETARDING GLUCOSE ABSORPTION

Iliyasu Datti Gwarzo[a], Siti Pauliena Mohd Bohari[a,c*], Roswanira Abdul Wahab[b,d]

[a]Department of Bioscience, Faculty of Science, Universiti Teknologi Malaysia, 81310 UTM Johor, Malaysia
[b]Department of Chemistry, Faculty of Science, Universiti Teknologi Malaysia, 81310 UTM Johor, Malaysia
[c]Cosmetic and Fragrance Laboratory, Institute of Bio-product Development, Universiti Teknologi Malaysia
[d]Advance Membrane Technology Research Centre, School of Chemical and Energy Engineering, Faculty of Engineering, Universiti Teknologi Malaysia, 81310 UTM Johor Bahru, Johor, Malaysia

Article history
Received
8 July 2024
Received in revised form
3 November 2024
Accepted
3 December 2024
Published Online
26 June 2025

*Corresponding author
pauliena@utm.my

Graphical abstract

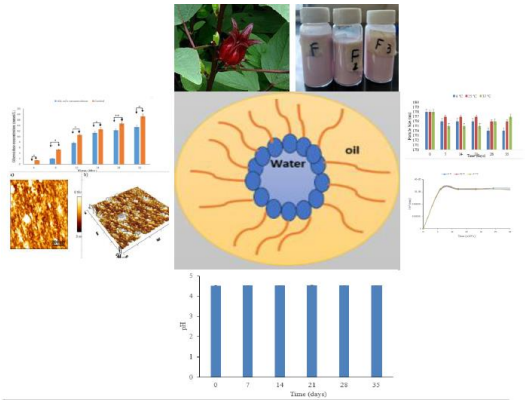

Abstract

Diabetes is the one of the prevalent non-communicable diseases, affecting millions across the globe. Conversely, conventional therapy involving blood glucose-lowering medications and insulin injections may lead to drug resistance or side effects because of the one-drug mechanism. *Hibiscus sabdariffa* Linn. (HSL) has the potential to maintain blood glucose levels and can be used along with the conventional treatment as an alternative approach. The phenolic components of HSL extract are very sensitive to environmental factors during processing and storage, resulting in low bioavailability and activity. Formulating the extract into a nanoemulsion extract is one technique to solve this problem. The best HSL water-in-oil nanoemulsion was achieved using 7% polyglycerol polyricinoleate (PGPR) surfactant, medium chain-length triglyceride (MCT): corn oil (1:1) which was subjected to different stability testing such as mean droplet size, polydispersity index, zeta potential, coalescent and Ostwald ripening. The *in-vitro* glucose release study using a dialysis tube revealed that HSL decreased the glucose diffusion to the outside solution (NaCl: 0.15M, 10 mL) by 44.12% after 24 hours. In short, the formulated HSL successfully resulted in the retarding of the release of glucose, conveying its potential use as a natural supplement for diabetic treatments.

Keywords: Diabetes, *Hibiscus sabdariffa Linn*, Nanoemulsion, Glucose, *in-vitro*

Abstrak

Diabetes adalah penyakit tidak berjangkit yang memberi kesan kepada berjuta manusia setiap tahun di seluruh dunia. Rawatan konvensional yang melibatkan ubat-ubatan untuk menurunkan glukosa di dalam darah dan suntikan insulin mempunyai risiko rentan atau kesan sampingan kerana mekanisma ubat tersebut. *Hibiscus sabdariffa Linn* (HSL) mempunyai potensi untuk meminimumkan tahap glukosa darah dan boleh digunakan bersama rawatan konvensional sebagai pendekatan alternatif. Walaubagaimanapun, komponen fenolik dalam ekstrak HSL sangat sensitif terhadap faktor persekitaran semasa pemprosesan dan penyimpanan, menyebabkan kesan Memformulasikan dan aktiviti yang rendah. Formulasi ekstrak ke dalam nanoemulsi adalah satu teknik untuk menyelesaikan masalah ini. Ekstrak HSL telah dihasilkan sebagai nanoemulsi air dalam minyak (w/o) menggunakan teknik bersepadu pencampuran tenaga yang lebih tinggi. Nanoemulsi air-dalam-minyak HSL terbaik diperoleh dengan menggunakan 7% surfaktan poligliserol polirisinoleat (PGPR), trigliserida rantai sedang (MCT): minyak jagung (1:1) yang diuji stabilitasnya melalui berbagai parameter seperti ukuran rata-rata tetesan, indeks polidispersitas, potensi zeta, penggabungan, dan pematangan Ostwald. Kajian pelepasan ubat secara *in-vitro* menggunakan tiub dialisis mendedahkan bahawa HSL w/o nanoemulsi mengurangkan penyebaran glukosa kepada cecair luar sebanyak 44.12% selepas 24 jam. Rumusannya, formulasi nanoemulsi ekstrak HSL w/o ini berjaya merencat perembesan glukosa, dan berpotensi sebagai makanan tambahan kesihatan semulajadi untuk rawatan penyakit diabetes.

Kata kunci: Diabetes, *Hibiscus sabdariffa Linn* (Roselle), Nanoemulsi, Glukosa, Ujian In vitro

1.0 INTRODUCTION

Diabetes mellitus (DM) manifests as a chronic condition arising from either the body's reduced efficiency in insulin utilization or insufficient production of this hormone by the pancreas, crucial for regulating blood sugar levels [1]. Moreover, diabetes also arises from certain diseases, malnutrition, genetic syndrome, or corticosteroid intake, which needs better medication [2]. According to the 9th edition of the International Diabetes Federation (IDF), diabetes has reached pandemic proportions, with a prevalence of 9% (463 million adults) in 2019 [3]. Also, it is estimated to rise to 693 million by 2045 worldwide [3]. Recent study showed that the number of diabetic patients in Malaysia is approximately 3.9 million, with 51% diagnosed and 49% undiagnosed [4].

To treat diabetes, a wide range of pharmaceuticals are used, including biguanides, thiazolidinedione, α-glucosidase inhibitors, sulfonylureas, and dipeptidyl peptidase-4 (DDP-4) inhibitors. [5, 6] exhibit side effects, such as cardiovascular diseases, gastrointestinal effects, weight gain, and glucopenia (a deficiency in any form of sugar) [7]. Furthermore, over the past three decades of significant advances using these oral antidiabetic agents, the outcome of these treatments is far from satisfactory due to several drawbacks including drug resistance (lower efficacy), harmful impacts, and even toxicity [8]. Due to this limitation, an alternative treatment based on natural products may provide benefits over synthetic drug [7].

Recently, there are reports on medicinal plants such as *Hibiscus sabdariffa* Linn., *Apium graveolens* and *Aloe vera*, for their promising use as natural treatments for diabetes [9, 10]. *Hibiscus sabdariffa* Linn. (HSL) specifically, has the dietary advantage that has to do with the bioavailability of its physiochemical properties, including flavonoids, especially anthocyanin. This Malvaceae family plant thrives in subtropical climates, such as those in India and Malaysia [11]. A study indicated that the two main flavonoid classes present in HSL, anthocyanins, are cyanidin-3-O-sambubioside and delphinidin-3-O-sambubioside [12]. The previously listed substances have been utilized to manage diabetes and other associated conditions like hyperlipidemia, obesity, overweight, and cardiovascular illnesses [12]. The mechanism of roselle (*Hibiscus sabdariffa Linn*.) extract as an antihyperglycemic drug was previously disclosed in our patent application (MY-193036-A), which shows how its synergistic effect has a more substantial effect than the sum of each individual effect [13]. However, maximal absorption of a high dose of the water-soluble roselle constituent to warrant its full antidiabetic benefit possesses a challenge, as the compound is quickly excreted by the human body through urine [14].

Nanoemulsion (NE) is a mixture of two liquids that are usually unable to mix together, such as water-in-oil

(w/o) or oil-in-water (o/w) droplets. It is stabilized by a suitable surfactant with a balanced hydrophilic-lipophilic profile (HLB) [15]. Nanoemulsion offers several advantages which include enhanced physiochemical properties higher stability due to smaller droplet size, improved biological activity, possesses drug carrier properties, and better bioavailability [16, 17]. In specifics, water-in-oil (w/o) and oil-in-water (o/w) nanoemulsions are the two main categories of nanoemulsions. w/o functional food formulation has already been utilized to shield antioxidants from plants [18]. However, this study only focused on formulating the water-in-oil nanoemulsion that will lower body glucose for antidiabetic patients. Water-in-oil (w/o) nanoemulsion is an emulsion in which a surfactant is used to highly homogenized the dispersion of water in an oil phase [19]. The stability of the w/o nanoemulsion makes it well-suited for the controlled release of active ingredients like anthocyanin from *Hibiscus sabdariffa Linn*. (HSL) throughout the gastrointestinal tract [20]. Food supplements in the form of w/o nanoemulsions containing naturally-extracted antidiabetic agents are likely alternative treatments to suppress hyperglycemic activity in diabetic patients [21]. Hence, an attempt was made to assess the w/o HSL nanoemulsion as a promising controlled-release delivery carrier through the digestive system for the anti-hyperglycemic effect.

2.0 METHODOLOGY

2.1 Materials

The dried fruit powder derived from *Hibiscus sabdariffa Linn. (HSL)* was procured from Bionutricia Manufacturing Sdn. Bhd (Selangor, Malaysia), while Sigma-Aldrich (St. Louis, MO, USA) provided the Folin-Ciocalteu phenol reagent. Analytical grade ethanol (99.86% mass fraction purity) was supplied by Hayman-Kimia (England), while medium-chain triglycerides (MCT) and Mazola maize oil were sourced from One-stop-shop in Johor Bahru, Malaysia. In the meantime, Biotek Abadi Sdn. Bhd., Selangor, provided the dialysis tube (MWCO 14000 Da), glucose colorimetric measurement kit, and human alpha-glucosidase.

2.2 *Hibiscus sabdariffa Linn.* (HSL) Fruit Extraction

A previously published methodology was followed to obtain the HSL fruit powder extract [22]. After being weighed using digital balance (Sartorius Quintix 3102-1s, Plasmas Enterprise Sdn Bhd, Germany), 100 g of HSL powder was added to a 1 L Erlenmeyer flask that had 70% v/v ethanol (1000 mL, 1:10 w/v). According to Paraíso *et al.* (2019), the mixture was sonicated for 45 minutes at a frequency of 20 kHz and 150 W in a cool ultrasonic bath (25°C). Afterward, the mixture was permitted to rest for a duration of 24 hours before undergoing filtration with a micro syringe filter with a pore size of 0.6 µm. To obtain the crude extract, any excess solvent was evaporated using a rotary evaporator (EYELA N-1000, Japan) under reduced pressure at 40°C. The concentrated sample was partitioned into multiple 50 mL falcon tubes, then subjected to lyophilization using ultra-cold freezer (UFZ-86V60E) for a duration of 48 hours and thereafter stored in a lightless condition at ambient temperature (27°C). The FTIR-ATR crude roselle extract spectrum was obtained using a Perkin-Elmer spectrophotometer (Frontier 100; USA) in One-bounce ATR mode. A Diamond/ZnSe crystal top plate containing 1.0 mg of crude roselle extract was used to build the spectrum in transmission mode at 16 scans and 4 cm^{-1} resolutions, spanning 400–4000 cm^{-1}.

The percentage yield of HSL crude extract was calculated according to Equation 1.

$$Yield\ (\%) = \frac{Weight\ of\ sample\ after\ freeze\ drying\ (g)}{Weight\ of\ dried\ sample\ (g)} \times 100\% \quad \text{(Equation 1)}$$

2.3 Bioactivities Testing

The lyophilized HSL calyces extract was subjected to phytochemical analysis, including the determination of total phenolic components, flavonoid content, and total anthocyanin. The analyses were conducted following the standard procedure reported by Rabelo *et al.* [23]. For the HSL water-in-oil nanoemulsion samples, each sample needs to be initially diluted with methanol to decrease its viscosity of the nanoemulsion. Afterwards, a process of centrifugation is carried out for a duration of 15 minutes at a speed of 10,000 rpm per minute using a Micro-centrifuge MX-307. (TOMY, Tokyo, Japan), prior to use.

2.4 Determination of Total Phenolic Compound

The Folin-Ciocalteu reagent was utilized to quantify the overall phenolic content (TPC) of the HSL extract or HSL without nanoemulsion. [22]. In a 96-well plate, the HSL extract and the HSL w/o nanoemulsion (10 µL, 20 mg/mL) were added. Next, 10% Folin-Ciocalteu reagent (10 µL) and 7.5% sodium trioxocarbonate (20 µL, 60 mg/mL) were added. The samples of the mixture mentioned above were shaken and then incubated for 30 minutes. The absorbance at 750 nm was measured using a microplate reader (Epoch-Biotech, Winooski, USA). Equation 2 was applied to calculate the total phenolic content (TPC), with the results expressed in milligrams of gallic acid equivalent (GAE) [24].

$$T = C \times \frac{V}{M} \quad \text{(Equation 2)}$$

In Equation 2, T(mg/100g) represents the Total Polyphenolic Content (TPC), V(ml), M (g) C represents the concentration of gallic acid obtained from the calibration curve, V represents the volume of the extract solution, and M represents the mass of the diluted sample extract.

2.5 Determination of Total Flavonoid Content

The aluminum chloride colorimetric method, as established by [24], was used to evaluate the total flavonoid content (TFC) in both the HSL extract and the HSL water-in-oil (w/o) nanoemulsion. 96-well plate was filled with the HSL extract or HSL w/o nanoemulsion (10 µL, 60 mg/mL), followed by ethanol (60 µL), distilled water (120 µL), 10% aluminum chloride (10 µL), and potassium acetate (1 M, 10 µL). After homogenizing the mixture, it was allowed to stand for 30 minutes. The absorbance of the solution was measured at 415 nm using a microplate reader (Epoch-Biotech, Winooski, USA). Results were expressed as milligrams of kaempferol equivalent (KE) per gram of extract (mg KE/g extract). Equation 3 was used to calculate the total flavonoid content.

$$C = C\frac{V}{m} \quad \text{(Equation 3)}$$

Equation 3 represents C (mgKE/g) as the total TFC, while C (mgKE/ml) represents the concentration of kaempferol from the calibration curve. The term V (ml) denotes the volume of the extract's solution and M (g) is the mass of the diluted extract.

2.6 Determination of Total Anthocyanin Content

The quantification of the total anthocyanin content (TAC) of the HSL extract or HSL water-in-oil (w/o) nanoemulsion was performed using the method described by [25], employing the pH differential approach. Two buffers were made using potassium chloride (0.025 M) and sodium acetate (0.40 M) to attain distinctive pH values of 1.0 and 4.5, respectively. Each 0.4 mL of HSL extract or HSL w/o nanoemulsion was added to 3.6 mL of buffer solution and transferred to a cuvette with a 1 cm path length. Absorbance measurements were conducted at 510 nm and 700 nm for pH 1.0 and pH 4.5, respectively, using a microplate reader (Epoch-Biotech, Winooski, USA), with water serving as the blank sample. The wavelength was determined utilizing this formula, which relies on the difference in absorbance [25], as shown in Equation 4.

$$A = Ab \times MW \times DF \times 1000/\varepsilon \times 1 \quad \text{(Equation 4)}$$

Ab in Equation 4 denotes for absorbance, MW refers to the molecular weight of cyanidin-3-glucoside (449.2 g mol^{-1}), DF is the dilution factor, ε represents the molar absorptivity of cyanidin-3-glucoside (26,900 L cm^{-1} mol^{-1}), and 1 describes the path length.

2.7 Quantification of Ethanol Content using Gas Chromatography–Flame Ionization Detector (GC-FID)

The ethanol concentration (mg/ml) of the sample was determined using the methodology described by Wang *et al.,* with some modifications. A 50% ratio of the mixture of ethanol (10% w/v) and HSL extract was mixed in a 1 mL capped vial. Then, the HSL extract and ethanol were injected into a chromatography machine equipped with FID detector (Agilent Technologies 6890N Network GC System, Germany). The ethanol recovery coefficient of variation (CV, %) was fixed at 15%. The quantification of ethanol was done by comparing the surface area of peaks belonging to ethanol and the HSL extract in relevance to the density of ethanol [26]. This was done to analyze the minimum ethanol content for halal consumptions.

2.8 Screening of Surfactant Concentration and Medium-Chain Triglycerides (MCT): Corn oil

A preliminary test was done to screen the variables, including surfactant concentration, dispersed phase, and oil concentration in the medium-chain triglycerides (MCT) and corn oil (CO) ratio. The HSL w/o nanoemulsion with the surfactant concentrations of 5% – 7% were screened for the lowest droplet size and polydispersity index (PDI). Different oil compositions were also analyzed for different oil ratios of medium-chain triglycerides (MCT) oil to corn oil (CO), MCT: CO at 1:0, 1:1, and 0:1.

2.9 Preparation of the W/O Nanoemulsion

The HSL water-in-oil (w/o) nanoemulsion is made by utilizing a combination of two potent emulsification processes, specifically high-pressure homogenization followed by ultrasonication. MCT oil and CO were utilized as the continuous phase, while the HSL extract, dissolved in ultrapure water, served as the dispersed phase in this formulation. Initially, a suitable concentration of polyglycerol polyricinoleate (7% PGPR) surfactant was added to the oil phase and stirred with a magnetic stirrer at 700 rpm and 80°C for 2 minutes before undergoing sonication for 5 minutes. Subsequently, the aqueous phase was introduced into the oil phase to prepare the coarse w/o emulsion, which was then homogenized using an ultra-homogenizer (15,000 rpm for 20 minutes; IKA T18 Digital Ultra Turrax, Germany). Finally, the coarse w/o nanoemulsion underwent ultrasonication using an ultrasonic processor (20-kHz, VCX 750 W, Sonics & Materials, Inc., Newtown, USA). Every sample was submerged in a cooled water bath sonicator, and ice was used to maintain the water batch's constant temperature of 30°C. The final w/o nanoemulsion was created by sonicating for one hour at an amplitude of sixty [27].

2.10 Physicochemical Analysis

Particle Size, Polydispersity Index, and Zeta Potential

The Malvern Instrument Zetasizer Nano (ZSP) from the United Kingdom was employed to determine the polydispersity index (PDI) and mean droplet size (MDS) of the water-in-oil (w/o) HSL extract nanoemulsion. Variations in temperature can modify the loading and

release rate of the bioactive component as well as the stability of the nanoemulsion. Therefore, at 25°C and a scattering angle of 173, all values were recorded. The substance was put into a capillary cuvette cell after being initially diluted (1:20) in deionized water. The zeta potential of each sample was determined at a temperature of 25°C using the ZetaSizer Nano Z.S. instrument manufactured by Malvern Instrument Ltd., UK. Zeta potential is a measurement of the ability of charged particles to move in an electric field. Prior to measurement, each sample was diluted with deionized water (1:200). All measurements were conducted in triplicate, and the results were reported as mean ± standard deviation (SD).

2.11 pH and Conductivity

The pH of the stable HSL extract-containing w/o nanoemulsion was monitored once a week for 35 days at room temperature (25 ± 0.5 °C) using a Delta 320 pH meter (Mettler Toledo USA). Prior to the measurement, the pH meter was calibrated by utilizing three pH standard buffer solutions with pH values of 4.0, 7.0, and 10.0. The conductivity test involved the use of a 0.01 M potassium chloride solution (KCl) and a conductometer (Mettler Toledo, USA) for calibration testing. Conductivity is used to quantify the presence of water and ions in a nanoemulsion (NE) in order to determine whether it is a water-in-oil (w/o) or oil-in-water (o/w) emulsion [28].

2.12 Atomic Force Microscopy

Atomic Force Microscopy (AFM) analysis was used to determine the Mean droplet size of the w/o nanoemulsion produced in this research. This test is required to acquire two- and three-dimensional visuals of the water droplets in the nanoemulsion as well as to validate the droplet size obtained by the prior dynamic light scattering (DLS) reading. The Just Plain Knight (JPK) data processing software system and the JPK Instrument NanoWizard® 3 Atomic Force Microscope (Berlin, Germany) were used to record the AFM utilising a significantly altered analysis approach [26]. After diluting the sample with ultrapure water, 10 µL of the diluted mixture was placed onto a small mica disc. the sample was then vacuum-dried to remove any leftover water. The instrument software was utilized to evaluate the photos collected during the tapping process.

2.13 Centrifuge Test, Freeze-thaw Cycle Test and Stability Test

The centrifugation test can be used to estimate a NE's shelf life in normal store settings. The freshly produced w/o nanoemulsion without the addition of roselle extract was subjected to centrifugation at a speed of 4000 rpm per minute for a duration of 15 minutes [27, 29]. Subsequently, the sample was analyzed to determine if any phase separation had occurred. The freeze-thaw stability test was then performed for three times, which involved the freezing and thawing processes and the holding process for each state (freeze state and room temperature state) for 24 hours before changing the environment. The physical features of a stable sample w/o HSL extract after the post-evaluation test should be identical to the pre-evaluated sample, without any separation of phases. Meanwhile, the MDS stability of the NEs was tested for 35 days at three different storage temperatures: 4℃, 27℃, and 37℃ [30, 31]. Temperature has a substantial impact on the stability of flaxseed oil nanoemulsions, with stability decreasing with higher temperatures [28].

2.14 Rate of Coalescence

Coalescence rate analysis was carried out to discover the factors that influence the variations in droplet size over time in a water-in-oil nanoemulsion containing the HSL extract. The droplet size data collected during the 35-day storage stability test at three different temperatures was calculated using Equation 5 (4°C, 25°C, and 40°C).

$$\frac{1}{r^2} = \frac{1x^2}{r^2 o} - [8\pi/3]\omega t \quad \text{(Equation 5)}$$

In Equation 5, the radius after time is denoted by r, the value at a specific time (s) is represented by ro, and the frequency of rupture per unit is indicated by t = 0. This study plotted the graph of $1r^{-2}$ versus storage time (s) to assess the rate of coalescence [30].

2.15 Rate of Ostwald Ripening

Ostwald ripening is a phenomenon where the size of nanoemulsion droplets grows due to the gradual diffusion of the oil phase into the aqueous phase. Use equation 6 to obtain the Ostwald ripening rate [32].

$$d^3 - d^3 o = \varpi = \frac{32}{9\alpha c D t} \quad \text{(Equation 6)}$$

Equation 6 represents ϖ (m^3/s)as the Ostwald ripening rate, α (=2γVm/RT), γ (N/m) is the interfacial tension, *Vm* (m^3/s) the molar volume of the lipid, *R* (J/(mol·K)) is the gas constant and *T* (K) is the absolute temperature, and finally, *c* (mol/m^3) is the water solubility of the lipid D (m^2/s) is the translational diffusion coefficient of the lipid in the water.

2.16 *In-vitro* Glucose Retardation Activity

The glucose release rate for HSL w/o nanoemulsion was evaluated using the glucose kit method developed by [33] with a slight modification, assuming that the transport in this system was aided by the convective activity of intestinal concentrations rather than simple diffusion. A dialysis tube with a molecular weight cut-off (MWCO) sized 14 kDa, 150 mm × 10 mm) was used as an *in-vitro* gastrointestinal tract model. The tube was

soaked in sodium chloride before used and then tightly tied on one side with a rubber band. In a dialysis tube containing 0.22 M D-glucose, the HSL w/o nanoemulsion (1 mL) was combined with NaCl (0.15 M, 1 mL). The dialysis tube's other end was knotted and put in a 50 mL centrifuge tube with 0.15 M NaCl (10 mL). In a shaker incubator (100 rpm), the tube was maintained at ambient temperature [34, 35]. The study aimed to assess the effect of HSL w/o nanoemulsion retarding on glucose diffusion by comparing it to pure water as the reference group. Measurements were taken at different time intervals (0, 4, 8, 12, 24, 28, and 32 h). Equation 7 was used to determine the glucose concentration that migrated into the external solution during the experiment using the glucose oxidase kit [33, 36].

$$C = Ab - Blank - c/m \quad \text{(Equation 7)}$$

C in Equation 7 represents the glucose concentration (mmol/L), Ab represents the absorbance of the sample, Blank represents the blank reading, c represents the intercept of the y axis, and m (m^3/mol) represents the gradient of the equation.

2.17 Statistical Analysis

The concentrations of bioactive substances, such as phenolic compounds, flavonoid content, and anthocyanins, were determined using Microsoft Excel. The findings revealed that these concentrations were within the expected mean range, with little variation compared to their mean levels. The flavonoid concentrations were 50.54 ± 1.88 mg KE/g and 40.66 ± 1.29 mg KE/g, respectively, demonstrating little dispersion around the mean. The pH readings were analysed using Excel, providing a mean of 4.53 ± 0.01, indicating minimal variability. However, the regulated glucose release data were statistically analysed with SPSS software. The analysis yielded statistically significant findings (p-value < 0.05).

3.0 RESULTS AND DISCUSSION

3.1 Ultrasonic Assisted Extraction of *Hibiscus sabdariffa Linn.*

This study yielded 22.8 g (22.8%) of *Hibiscus sabdariffa* Linn. fruit extract *via* ultrasonic-assisted extraction (UAE). The yield was found to be higher compared to the one extracted by maceration [37]. Similarly, Peredo-Pozos *et al.* [38] compared the efficiency of extracts of HSL yielded from ultrasonic-assisted extraction (UAE) with the conventional method and found that UAE provides a higher yield of 20.84g while conventional yielded 13.74g [38]. This suggests that UAE is well suited for the extraction of bioactive HSL compounds as it provides a high extract. sonication enhances hydration and fragmentation of the material, facilitating mass transfer without significant solvent decomposition [38].

3.2 Bioassay Analysis

3.2.1 Total Phenolic Compound (TPC)

The quantification of total phenolic compounds (TPC) was performed by utilizing a standard calibration curve of Gallic acid. The TPC was determined as gallic acid equivalent (GAE) with R^2 value of 0.98. The HSL extract and HSL water-in-oil (w/o) nanoemulsion had total phenolic compounds of 29.30 ± 0.5 mgGAE/g and 22.30 ± 0.5 mgGAE/g, respectively (Table 1). The reduction in the content was likely a result of their susceptibility to various environmental factors, such as light and heat, which led to their degradation [39].

Table 1 Bioassay Compounds of HSL Extract and HSL w/o nanoemulsion

Bioassay Compound	HSL Extract	HSL w/o nanoemulsion
TPC (mgGAE/g)	29.30 ± 0.5 gGAE/g	22.30 ± 0.5 mgGAE/g
TFC (mgKE/g)	50.54 ± 1.88 mgKE/g	40.66 ± 1.29 mgKE/g
TAC (mg/100g)	367.82 ± 0.25mg/100g	323.70 ± 0.52mg/100g

3.2.2 Total flavonoid Content (TFC)

This research quantified total flavonoid content using kaempferol as the standard calibration curve as they have the same chemical groups as quercetin. The standard curve showed that the R^2=0.98 and the total flavonoid content of the HSL extract and HSL w/o nanoemulsion were 50.54 ± 1.88 mgKE/g and 40.66 ± 1.29 mgKE/g, respectively (Table 1). As expected, reduce concentration of flavonoids in HSL w/o nanoemulsion was caused by the fact that these compounds are heat- and light-sensitive [40]. While the concentration of TFC in HSL w/o nanoemulsion was lower compared to the HSL extract, previous research has shown that the TFC content in extracts from different cultivars ranges from 22.6 to 41.92 mgQE/g [41-43]. Therefore, it can be said that TFC concentration for HSL w/o nanoemulsion is still within a desirable range compare to other source of extract [38].

3.2.3 Total Anthocyanin Content (TAC)

The anthocyanin content of this study was found to be 367.82 ± 0.25 mg per 100 g dry weight while the anthocyanin contents of HSL w/o nanoemulsions were found to be 323.70 ± 0.52 milligrams per 100 g dry weight (Table 2). Similarly, [23] reported a decrease in anthocyanin content when formulating a water-in-edible oil nanoemulsion [23]. A higher rate of deterioration was noted for anthocyanin in w/o nanoemulsion compared to anthocyanin of the extract, with all values being statistically different ($p < 0.05$) [23]. This result also fell in the range of other studies which indicated the HSL fruit has TAC ranges from 303.02

mg/100g to 1883 mg/100g depending on the genotypes of the fruits [43].

3.3 Fourier Transform Infrared Spectroscopy–Attenuated Total Reflection (FTIR-ATR)

This study is often used to determine the fingerprint of a molecule as well as functional groups and their interactions [15]. The active functional group was detected in both HSL extract and HSL w/o nanoemulsion using FTIR-ATR analysis, as circled in red, and the peaks are represented in Figure 1a and 1b. The peak assignment to the corresponding functional groups is summarized in Table 2. The FITIR confirmed the presence of the bioactive compound.

Table 2 FTIR-ATR Peaks of the HSL Extract for Their Bioactive Compounds

Bioactive compounds	Peaks (found) (cm^{-1})
Phenolic compound	3100-3500, 2854, 2924
Flavonoid compound	1782.53, 1786, 1742
Anthocyanin compound	1188.16, 1019.07, 1103, 1157.0

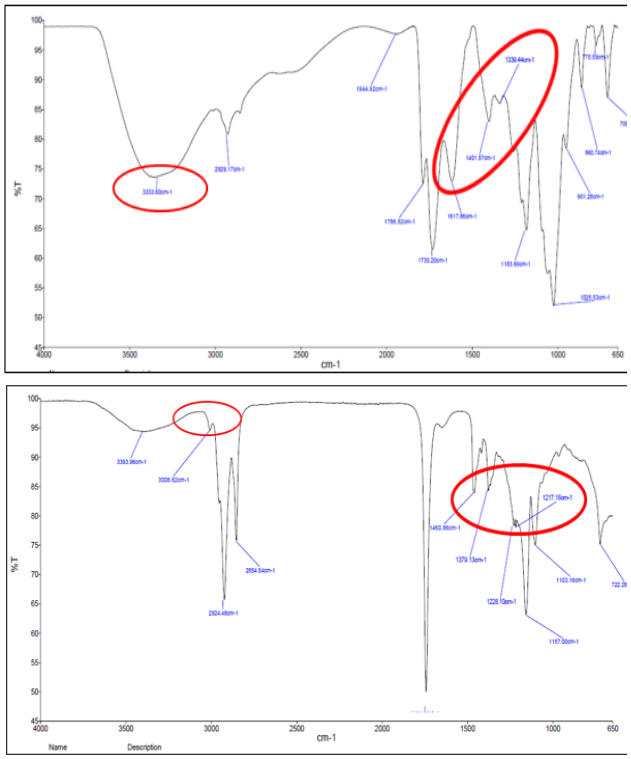

Figure 1 The FTIR-ATR profile of the a) HSL extract and the b) HSL w/o nanoemulsion

3.4 Total Ethanolic Present in the Extract

This study used gas chromatography in conjunction with flame ionization detection (GC-FID) to determine the total quantity of ethanol contained in the HSL extract. This study measured the amount of ethanol to determine that the extract is halal for consumption. Figure 2 shows the GC profiles of ethanol and the extract. The ethanol was calculated by comparing the value of the surface area for the ethanol profile peak with the value of the surface area for the HSL extract profile peak found in the retention time of 1.774 (Figure 2). The result showed that only 0.02% of ethanol remained in the sample which is far below the one percent (1%) benchmark. The percentage of acceptable ethanol must be between 0.1% and 1% to meet the Halal Certification Body guidelines (HCB) [45]. Hence, this extract is suitable for halal food production [44].

Several prominent Halal Certification Bodies (HCBs), including the Islamic Religious Council of Singapore (MUIS), the Assessment Institute for Foods, Drugs, and Cosmetics of the Indonesian Council of Ulama (LPPOM MUI), and the Department of Islamic Development Malaysia (JAKIM), have set specific limits for the amount of permissible ethanol in Halal foods and beverages. These cutoff points range from 0.1% to 1%, contingent upon the HCB [44, 45]. Therefore, this study ensured that the ethanol in the extract was vacuum evaporated to the acceptable level for Halal food.

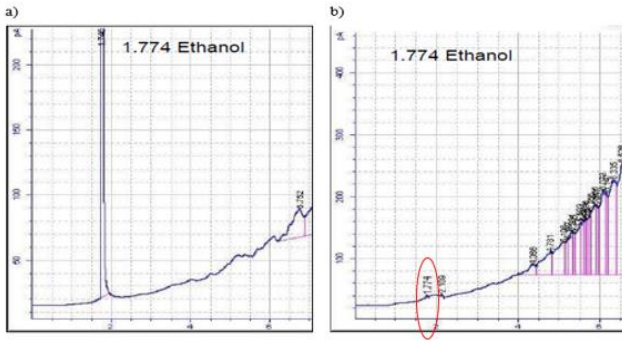

Figure 2 GC-FID profile of a) Standard ethanol and b) extract

3.5 Screening of the Formulation Variables

This study initially screened the composition of the primary nanoemulsion to evaluate the appropriateness of its components and identify the elements that impact the ultimate quality of the nanoemulsions. Prior to the main formulation, a ratio of the surfactant concentration and the oil concentration in MCT oil and corn oil CO were screened successfully. This study selected PGPR surfactant because of its low ionic value that favors interaction within the water-in-oil nanoemulsion. PGPR is a common place surfactant in food-grade formulations [27]. Based on the screening investigation utilizing centrifugation and freeze-thaw cycles (Table 3), the formulations employing MCT oil and a mixture of MCT oil and CO were stable, whereas those using solely CO were unstable. Formulation using solely CO was unstable as corn oil has a high monounsaturated fatty acid content requiring a higher surfactant concentration for better emulsification [29]. Conversely, MCT containing fewer monounsaturated

fatty acids needed a modest amount of surfactant to create a stable nanoemulsion [29]. It appears that a mixture of MCT and CO was the better choice to produce a stable nanoemulsion. Thus, the mixture of MCT oil and CO was selected for further formulation in this work.

The study revealed that the water-in-oil (w/o) HSL extract formulation resulted in a mean droplet size (MDS) ranging from 178 to 395 nm, with a satisfactory polydispersity index (PDI) between 0.3 and 0.5 (Table 3). This range corresponds to varying surfactant concentrations (5% – 7%), with lower concentrations resulting in higher MDS and vice versa (Table 3). The study found that using 7% PGPR was suitable to yield a low MDS (178 nm) in the w/o HSL extract nanoemulsion. Thus, well accepted within the recommended range for droplet size in a nanoemulsion [46]. Another factor in determining the optimum nanoemulsion is the polydispersity index (PDI) which showed the mono dispersity or the polydispersity of the system. Results revealed that the HSL w/o nanoemulsion was monodispersed as reflected in the PDI ranges from 0.3 – 0.5 (Table 3). Literature has shown that a PDI value of 0 (zero) signifies a monodispersed system, while the value of 1 is a polydisperse one [47]. Based on the collective results, the suitable composition to prepare the HSL w/o nanoemulsion using a combination of MCT and CO (MCT: CO, 1:1) as the best oil composition, with 7 % (w/w) PGPR as the surfactant, to give MDS and PDI values of 178 nm and 0.330, respectively. Thus, the outcome affirmed that the study's goal was to produce the w/o HSL extract MDS < 200 nm has been achieved.

3.6 Physicochemical Characterization of w/o HSL Extract Nanoemulsion

3.6.1 Mean Droplet size (MDS) and Polydispersity Index (PDI)

The quality, the homogeneity, and the dispersibility of nanoemulsions are largely determined by the distribution of their particle sizes, mean particle diameters (Z-averages), and polydispersity indices (PDI). It's important to emphasize that nanoemulsions characterized by small droplet sizes and low polydispersity index (PDI) are highly desirable for ensuring a long shelf life [43]. Figure 3 illustrates the particle size distribution of the optimal water-in-oil (w/o) HSL extract nanoemulsion, revealing a mean droplet size (MDS) of 178 nm. Similarly, [23] developed an Açaí berry w/o nanoemulsion with MDS ranging from 146.8 to 814.8 nm and observed that a lower MDS (146.8 nm) conferred greater kinetic stability compared to higher MDS variants [23]. Moreover, the smallest MDS will facilitate the delivery of the w/o HSL nanoemulsion extract through the gastrointestinal tract (GIT) efficiently [48].

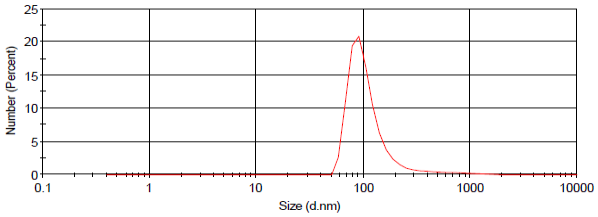

Figure 3 Size profile of HSL w/o nanoemulsion

As described, the PDI of the HSL w/o nanoemulsion was found to be 0.301, suggesting the monodispersity of the system. A monodispersed formulation must have clear, homogenous similar-sized droplets for effective delivery [49]. Moreover, a low PDI value suggests nanoemulsion stability over a long period, which is critical for the controlled release of HSL w/o nanoemulsion in the human gastrointestinal tract [50]. Additionally, it is essential for the formulation to use a controlled release method to avoid uneven drug release at a specific time. In short, based on the combined low MDS and the mono dispersity of the HSL extract w/o nanoemulsion, the formulation may be adequately robust and has a long shelf life [51].

3.6.2 Zeta Potential

A zeta sizer is utilized to assess the charge stability of the nanoemulsion, reflecting the surface charge functionality of the droplets [42]. The sample was loaded into a zeta cuvette and droplet measurements were recorded in millivolts (mV) [42, 46]. The zeta potential of the water-in-oil (w/o) HSL extract nanoemulsion in this study was determined to be -40.02 mV (Figure 4). The result also implied a kinetically stable w/o system with presumably an extended shelf life and the ability to resist destabilization by coalescence or Ostwald ripening [52]. This was because the two types of oil employed (MCT and CO) might yield a lower zeta potential (-40.02 mV).

Similarly, [53] found that their formulated water-in-olive oil nanoemulsions with the lowest zeta potential were exceptionally stable, resulting in longer shelf life [53]. A zeta potential between ±30 mV is typically sufficient to guarantee the physical stability of nanoemulsions. The study found that the ideal water-in-oil (w/o) HSL extract nanoemulsion had a negative charge, as shown in Figure 4. This suggests that the nanoemulsion was stabilized by Van der Waals electrostatic repulsion. Consequently, the nanoemulsion can be expected to maintain stability over an extended period [49].

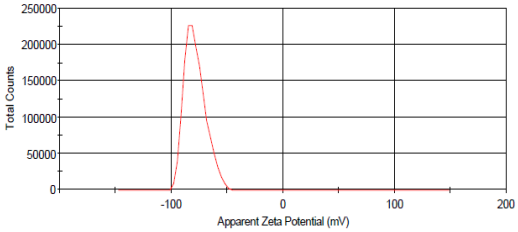

Figure 4 The zeta potential distribution of HSL nanoemulsion

3.6.3 pH Measurement

pH is a measure of the acidity or alkalinity of a substance [50]. The objective of this study was to verify the safety of a water-in-oil (w/o) HSL nanoemulsion for consumption. The optimized nanoemulsion showed an average pH of 4.53 ± 0.01 indicating stability and no signs of microbial contamination as shown in Figure 5. The pH level of 4.53 is low enough to inhibit the growth of many pathogenic microorganisms, which typically prefer a neutral pH environment. This indicates that the nanoemulsion is less likely to support microbial growth, which is crucial for ensuring the product's safety for consumption. The absence of microbial contamination suggests proper formulation and storage conditions [54]. The pH range of an oral quercetin-loaded nanoemulsion is 4.0 − 9.0 [55]. Thus, this study achieved its goal to prepare the HSL w/o nanoemulsion adhering to conditions that guarantee an extended shelf and safety for consumption.

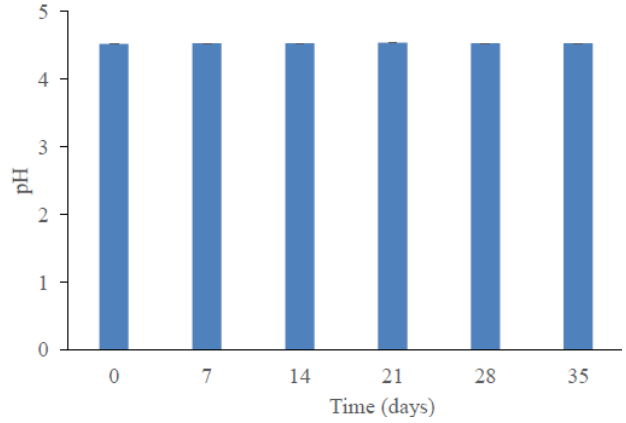

Figure 5 pH value of HSL w/o nanoemulsion for 35 days

3.6.4 Conductivity

Conductivity tests was performed to determine if the optimized water-in-oil (w/o) HSL nanoemulsion was an oil-in-water (o/w) or water-in-oil (w/o) colloidal dispersion system. It is important to note that an oil-in-water (o/w) system typically has a higher conductivity than a water-in-oil (w/o) system, because the former has water in the exterior phase [49, 51]. In this perspective, the conductivity of the formulated w/o HSL extract nanoemulsion found to be 0 S/m which proved that the HSL extract is water-in-oil nanoemulsion. Moreover, another study proved that the canola w/o nanoemulsion has lower conductivity (0.038 S/m) to confirm it is w/o [56]. The low conductivity of the HSL w/o nanoemulsion conveys oil being its primary composition, hence the poor conductivity. Larger conductivity, on the other hand, is attributed to higher water concentrations, which allow ions to move freely [57]. The zero conductivity of the w/o HSL extract nanoemulsion was due to the low composition of water (18 %) in the formulation, and this aqueous system is encapsulated by oil [56]. This proved that the nanoemulsion containing HSL extract was water-in-oil [31]. Similarly, another study shows that canola w/o nanoemulsion showed a conductivity of 0.038 S/m [56].

3.6.5 Atomic Force Microscopy (AFM)

Atomic force microscopy (AFM) is a modern method used to observe the surface structure of nanoemulsion formulations. AFM analysis provides a simpler and more user-friendly alternative to Scanning Electron Microscopes (SEM) and Transmission Electron Microscopes (TEM). It enables observation of the droplet interface under conditions closely resembling those in actual nanoemulsions [43, 53].

Two reference points (Figures 6c(ii) and d(ii)) were chosen, where the vertical distance (height difference) was nearly identical for the reliability of the droplets cross-section topography. The height profile can be used to confirm the height and the size of the highlighted atom [58]. The AFM micrographs of the optimum HSL w/o nanoemulsion revealed that the spherically shaped droplets were distributed in sizes of < 200 nm confirming the size obtained by zeta size instrument (Figure 6a). Moreover, the three-dimensional topographies (Figure 6b) show the cross-section length of the droplets, with diameters between 92.50 − 142.6 nm. Likewise, the AFM 2D micrograph (Figures 6c(i) and d(i)) corroborated the nano-sized particles within the w/o HSL nanoemulsion. Figures 6c(ii) and d(ii) depict the height profiles of the selected droplets, respectively.

Finally, the results of the AFM micrographs corresponded well to the previous results of the MDS from DLS (178 nm), the former showing the MDS of the HSL w/o nanoemulsion < 200 nm. However, it can be construed that the optimum HSL w/o nanoemulsion shows good physicochemical properties to support its slow release of the HSL extract in the human gut.

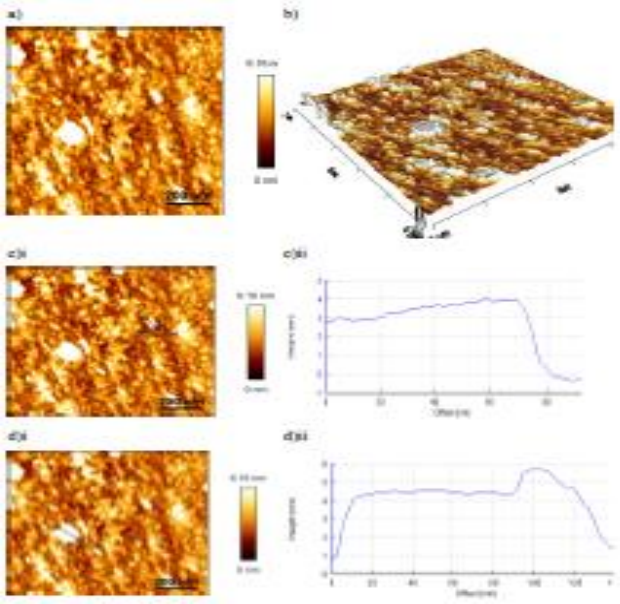

Figure 6 AFM images of the optimal HSL w/o nanoemulsion a) error signal of 1 1 µm² area (b) 3D topography of 1 x 1 µm² area, c)i, and d)i 2D topographies and c)ii and d)ii are height profiles of the selected water droplets

Table 3 Screening of variables for the optimal w/o HSL extract formulation

MCT (%)	CO (%)	Surfactant (%)	Deionized water (%)	HSL extract (%)	Sweetener (%)	Centrifugation	Freeze-thaw Cycle	MDS (nm)	PDI
36.5	36.5	5	18	2	2	√	√	395	0.453
36	36	6	18	2	2	√	√	265.9	0.385
35.5	35.5	7	18	2	2	√	√	178	0.330
73	0	5	18	2	2	√	√	390	0.411
72	0	6	18	2	2	√	√	260.3	0.330
71	0	7	18	2	2	√	√	180	0.301
0	73	5	18	2	2	×	×	×	×
0	72	6	18	2	2	√	×	×	×
0	71	7	18	2	2	√	×	×	×

√= stable (no separation)
× =unstable (separation phase)

3.7 Accelerated Stability Study

A nanoemulsions stability is investigated through stability tests to assess how it will react to changes in temperature, humidity, and light [59]. Stability tests for nanoemulsion were performed by storing the formulation for 35 days under several conditions: room temperature, elevated temperature, and freezing, in accordance with the guidelines set by the International Conference on Harmonization [60]. The thermodynamic stability of the ideal nanoemulsion was investigated in this study through a variety of extreme storage environments including centrifugation, freeze-thaw cycles, and cryogenic freezing. When storing a nanoemulsion, it is useful to know how long it will last. Henceforth, the formulated HSL nanoemulsion was centrifuged to confirm there is no separation in the nanoemulsion. The findings

indicate that there was no occurrence of phase separation during the 35-day storage period, as depicted in Figures 7a and 7b.

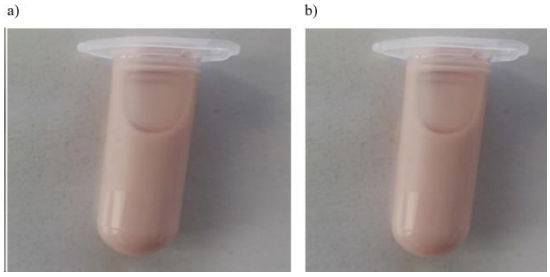

Figure 7 phase separation of nanoemulsion a) before centrifugation and b) after centrifugation

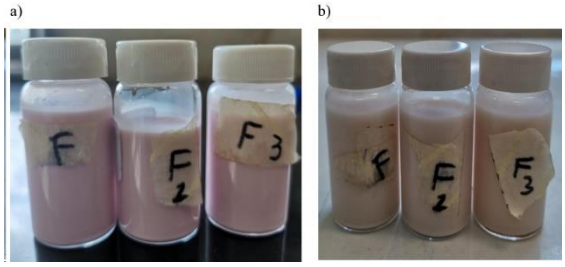

Figure 8 a) The HSL w/o nanoemulsion at 0 days and b) after 35 days of storage

Additionally, although the freeze-thaw cycle was performed six times, phase separation remained undetectable after 35 days of storage at various temperatures (4°C, 25°C, and 37°C). However, Figures 8a and 8b show diminishing coloration over some time. This may likely be because anthocyanin, which is responsible for the color, start to deteriorate when exposed to light [61]. Table 4 shows that the formulations have passed the stability test based on the storage time and centrifugation and appeared adequately stable for subsequent investigations.

Table 4 Accelerated Stability of HSL w/o nanoemulsion

Temp	Storage stability					
	0 week	1st week	2nd week	3rd week	4th week	5th week
4 °C	√	√	√	√	√	√
25 °C	√	√	√	√	√	√
37°C	√	√	√	√	√	√

√ Stable (No phase separation)

3.8 Long-term Storage and Stability

3.8.1 Monitoring of Mean Droplet Size and Polydispersity Index

The durability of a formulation is mostly dictated by the stability of the formulated nanoemulsions. In order to evaluate the ability of the nanoemulsion sample to resist coalescence and Ostwald ripening, the mean droplet size (MDS) and polydispersity index (PDI) were measured after storing the sample at temperatures of 4°C, 25°C, and 37°C. Figures 9a and 9b illustrate the changes in MDS and PDI of the optimal nanoemulsions after 35 days of storage at different temperatures. The MDS ranged from 178 to 174 nm, while the PDI fluctuated between 0.27 and 0.308. Initially, on the first day of preparation, the MDS and PDI of the ideal nanoemulsion were slightly higher (MDS = 178 nm, PDI = 0.303) compared to samples stored for 35 days (Figure 9). This behavior suggests that the colloidal dispersion system had not yet settled and reached equilibrium. Samples kept at 4°C exhibited lower MDS and PDI (MDS = 174 nm, PDI = 0.269), followed by those stored at 25°C (MDS = 176 nm, PDI = 0.300). Storage at 37°C appeared to be more destabilizing, resulting in an MDS and PDI value of 177 nm and 0.299, respectively. This destabilization could be attributed to water loss, which may promote coalescence of the water-in-oil HSL nanoemulsion. The MDS of the ideal nanoemulsion remained around 175 nm until the 35th day, indicating good stability. However, the immediate increase in MDS of the HSL w/o nanoemulsion at 25°C and 37°C storage may be due to either coalescence or Ostwald ripening. Nevertheless, the sudden rise in mean droplet size (MDS) of the hydrophobic solvent (HSL) without nanoemulsion after storage at 25°C and 37°C might be attributed to either coalescence or Ostwald ripening. Similar studies have also demonstrated a consistent trend, confirming that the observed decrease was not influenced by coalescence [59, 62]

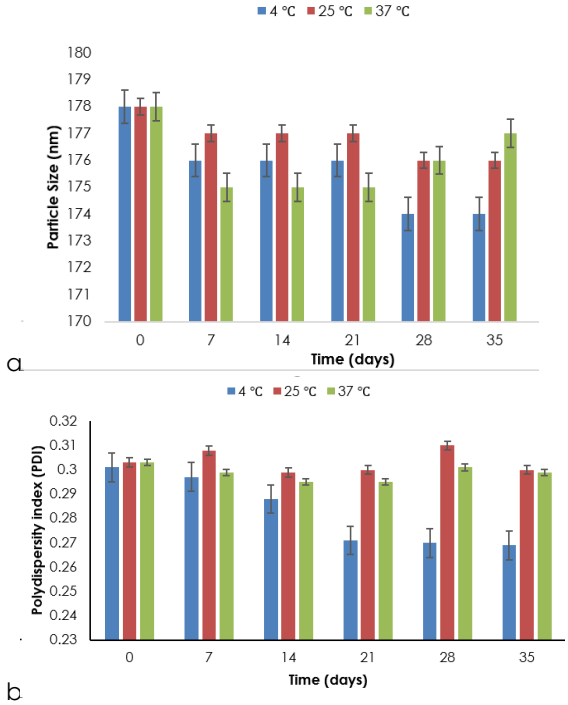

Figure 9 Physical stability of the HSL extract w/o nanoemulsion in terms of a) MDS and b) PDI

3.8.2 Rate of Coalescence

Nanoemulsions, unlike microemulsions, have enhanced resilience to a range of storage instabilities such as coalescence, creaming, sedimentation, flocculation, and Ostwald ripening [63]. Over time, collisions between the minute water droplets within the optimized nanoemulsion may lead to coalescence, resulting in phase separation and an increase in mean droplet size (MDS) over an extended period, thereby affecting storage stability. Figure 10 illustrates the graph of 1/r^2 versus storage duration, indicating that droplet sizes for the water-in-oil (w/o) HSL extract nanoemulsion stored at 4°C, 25°C, and 37°C were not linear. Notably, droplet sizes decreased for samples stored at 4°C, suggesting greater stability at this temperature. The overall trend suggests that the change in MDS over time was not primarily due to coalescence. This study observed that reducing the storage temperature improved the emulsions' resistance to droplet coalescence [59].

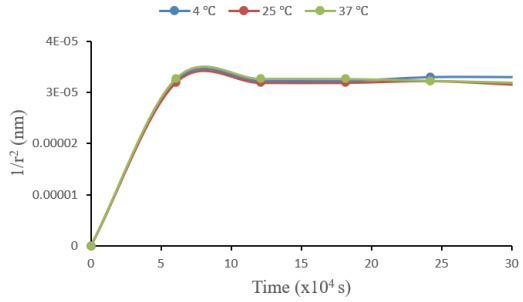

Figure 10 Rate of coalescence for the HSL w/o nanoemulsion stored at various temperatures

3.8.3 Rate of Ostwald Ripening

Ostwald ripening is a process in which an emulsion undergoes the growth of larger droplets at the cost of smaller ones, caused by the molecular diffusion of oil between droplets in the continuous phase [57]. Figure 11 illustrates the change in droplet size from 175 nm on day 7 to 178 nm on day 35, plotted against storage duration. Samples stored at 4°C showed no significant impact from Ostwald ripening, as evidenced by the decrease in mean droplet size from 178 nm on day 1 to 174 nm on day 35, indicating stability. The stability of the system was ascribed to the solubility of the oil employed, namely medium-chain triglycerides and coconut oil. In contrast, long-chain triglycerides such as corn oil, which are not soluble in water, hindered the occurrence of Ostwald ripening [57]. Additionally, temperature directly influences particle motion [58]. The samples held at 25°C and 37°C showed an increase in the average size of droplets. This is probably because the dispersed droplets moved more vigorously through the continuous phase at higher temperatures, resulting in more collisions between droplets and hence an increase in size [58]. The ideal nanoemulsion's r^3 value appeared to plateau, indicating no significant effect from Ostwald ripening during storage. The surfactant effectively prevented Ostwald ripening in the water-in-oil (w/o) HSL nanoemulsion by inhibiting water droplet diffusion into the continuous oil phase [64]. Similar behavior was observed in a curcumin-loaded medium-chain triglycerides (MCT) nanoemulsion that utilized a blend of emulsifiers Sorbitan monooleate/Span 80 to delay Ostwald ripening phenomena in the MCT oil phase [65].

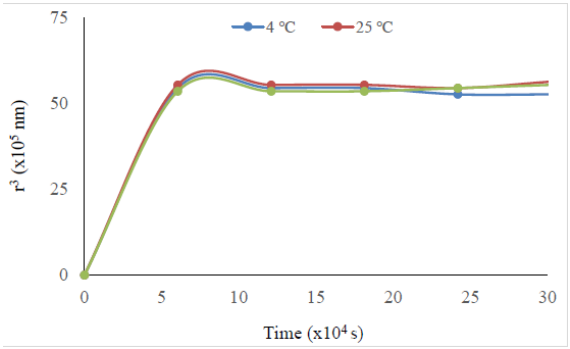

Figure 11 The rate of Ostwald ripening on the HSL extract w/o nanoemulsion held at various temperatures

3.9 *In-vitro* Controlled Glucose Release Study of HSL w/o Nanoemulsion

In in-vitro controlled release experiments of nanoemulsions containing active medications, a dialysis tube can serve as a tool for analysis. This method offers a straightforward framework for evaluating the ability of soluble dietary fibers to impede the movement and spread of glucose in the intestines. Mechanistically, this research aimed to inhibit the diffusion of glucose, and the nano-sized nanoemulsion led to the requirement of higher MWCO cut-up [66, 67]. A glucose oxidase kit was used to determine the amount of glucose released. HSL w/o nanoemulsion led to a restrain release of glucose at 4, 8, 12, 24, 28, and 32 h intervals (Figure 12). The result of the present study indicated that HSL led to an inhibitory effect on the metabolism of glucose. Timely glucose release is a critical aspect of a therapeutic system for drug delivery so that the actual time for absorption of the therapeutic agent be known [68].
HSL w/o nanoemulsion retards the glucose diffusion through the dialysis tube (Figure 12). At different time intervals, HSL w/o nanoemulsion was found to be significantly inhibiting glucose diffusion versus control ($p < 0.05$), except at 28 h ($p > 0.05$) (Figure 12). There was a 0.001 ± 0.0001 mmol/L of glucose in the beaker after 4 h, indicating that glucose was inhibited from leaving the tube to the environment (Figure 12). Furthermore, the rate of glucose diffusion into the environment increased significantly from 8 to 32 hours. After 24 hours of monitoring, HSL w/o nanoemulsion prevented 44.12% of glucose from diffusing into the environment (sodium chloride solution). [13] employed a pure HSL extract and obtained a 95%

glucose inhibition after 24 hours. The discrepancies could be attributed to different molecular weights cut off from the dialysis tube, pure extract, nanoemulsion concentration, and encapsulated extract [69]. The HSL w/o nanoemulsion was found($p<0.05$) for 4,8,12, 24 and 28 h significant in inhibiting glucose diffusion outside the dialysis tube. Regulating postprandial blood glucose levels is an essential aspect of managing diabetes. It is frequently employed as a clinical metric to forecast the probability of getting diabetes. The findings also indicated that the formulated HSL could serve as a natural oral supplement for those with diabetes.

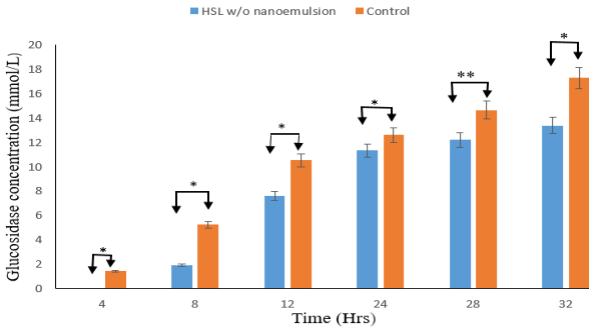

* $p< 0.05$, ** $p> 0.005$ *compared to the control*

Figure 12 The effect of HSL w/o nanoemulsion on the time-dependent glucose diffusion from a sealed dialysis tube into the outside solution

4.0 CONCLUSION

The study successfully formulated the water-in-oil nanoemulsion. Ultrasonic-assisted extraction (UAE) was successfully used to extract the bioactive compound of *Hibiscus sabdariffa* Linn. It yielded an extract of 22.8% containing total phenolic compound of 29.30 ± 0.5 mgGAE/g, total flavonoid content of 50.54 ± 1.88 mgKE/g and total anthocyanin content of 367.82 ± 0.25SD mg/100 g. FTIR-ATR was used to analyze the presence of these bioactive compounds, detecting flavonoids and anthocyanins at the waves of 1782 cm^{-1} and 1103 cm^{-1}, respectively. Corn oil and medium-chain triglycerides (MCT) oil were mixed with PGPR surfactants and HSL extract as an aqueous phase to formulate a hydrogel prepared by homogenization and ultrasonic treatment. The HSL water-in-oil nanoemulsion demonstrated stability without phase separation throughout accelerated stability tests involving centrifugal force and freeze-thaw cycles, as well as during long-term storage at temperatures of 4°C, 25°C, and 37°C for a duration of up to 35 days. According to a dialysis tube-based *in-vitro* investigation of glucose release, the HSL reduced glucose diffusion by 44.12% after 24 hours. The findings indicated that any drugs that prevent glucose from diffusing in the digestive tract can regulate postprandial blood glucose. In short, the formulated HSL w/o nanoemulsion successfully resulted in the time-manner release of the glucose, conveying its potential use as a natural supplement to maintain blood glucose level. However, molecular modelling and dynamic simulation are recommended to understand better the mechanism and the drug loading mechanism of the formulated HSL extract w/o nanoemulsion

Acknowledgment

The authors extend their appreciation to the Department of Bioscience, Faculty of Science, Universiti Teknologi Malaysia, for providing their facilities. This research was supported by the Ministry of Education (MOE) through the Fundamental Research Grant Scheme (FRGS/1/2020/STG01/UTM/02/8) with grant no. R.J130000.7754.5M006.

Conflicts of Interest

The author(s) declare(s) that there is no conflict of interest regarding the publication of this paper.

References

[1] V. Leso, I. Capitanelli, E. A. Lops, W. Ricciardi, and I. Iavicoli. 2017. Occupational Chemical Exposure and Diabetes Mellitus Risk. *Toxicology and Industrial Health*. 33(3): 222–249.

[2] D. R. Whiting, L. Guariguata, C. Weil, and J. Shaw. 2011. IDF Diabetes Atlas: Global Estimates of the Prevalence of Diabetes for 2011 and 2030. *Diabetes Research and Clinical Practice*. 94(3): 311–321.

[3] H. Sun *et al.* 2022. IDF Diabetes Atlas: Global, Regional and Country-level Diabetes Prevalence Estimates for 2021 and Projections for 2045. *Diabetes Research and Clinical Practice*. 183: 109119.

[4] M. Osman and N. M. Zain. 2021. Knowledge and Practices of Cardiovascular Diseases Prevention Among Patients With Type 2 Diabetes Mellitus at Hospital Universiti Sains Malaysia. *International Journal of Care Scholars*. 4(1): 18–28.

[5] B. Salehi *et al.* 2019. Antidiabetic Potential of Medicinal Plants and Their Active Components. *Biomolecules*. 9(10): 551.

[6] S. Tian *et al.* 2013. Modeling Compound–Target Interaction Network of Traditional Chinese Medicines for Type II Diabetes Mellitus: Insight for Polypharmacology and Drug Design. *Journal of Chemical Information and Modeling*. 53(7): 1787–1803.

[7] W. Li, G. Yuan, Y. Pan, C. Wang, and H. Chen. 2017. Network Pharmacology Studies on the Bioactive Compounds and Action Mechanisms of Natural Products for the Treatment of Diabetes Mellitus: A Review. *Frontiers in Pharmacology Review*. 8(74).

[8] M. U. Rao, M. Sreenivasulu, B. Chengaiah, K. J. Reddy, and C. M. Chetty. 2010. Herbal Medicines for Diabetes Mellitus: A Review. *Int J PharmTech Res*. 2(3): 1883–1892.

[9] M. Koala *et al.* 2021. HPTLC Phytochemical Screening and Hydrophilic Antioxidant Activities of *Apium graveolens L., Cleome gynandra L., and Hibiscus sabdariffa L*. Used for Diabetes Management. *American Journal of Analytical Chemistry*. 12(01): 15.

[10] I. D. Gwarzo, S. P. Mohd Bohari, R. Abdul Wahab, and A. Zia. 2022. Recent Advances and Future Prospects in Topical

Creams from Medicinal Plants to Expedite Wound Healing: A Review. *Biotechnology & Biotechnological Equipment*. 36(1): 81–93.
[11] F. Tavakolifar, M. H. Givianrad, and M. Saber-Tehrani. 2016. Extraction of Anthocyanins from *Hibiscus sabdariffa* and Assessment of Its Antioxidant Properties in Extra Virgin Olive Oil. *Fresenius Environ. Bull*. 25: 3709–3713.
[12] F. Les, G. Cásedas, C. Gómez, C. Moliner, M. S. Valero, and V. López. 2020. The Role of Anthocyanins as Antidiabetic Agents: From Molecular Mechanisms to in Vivo and Human Studies. *Journal of Physiology and Biochemistry*. 1–23.
[13] R. M. Shadhan and S. P. M. Bohari. 2017. Effects of Hibiscus Sabdariffa Linn. Fruit Extracts on a-glucosidase Enzyme, Glucose Diffusion and Wound Healing Activities. *Asian Pacific Journal of Tropical Biomedicine*. 7(5): 466–472.
[14] S. Pimentel-Moral, C. Rodríguez-Pérez, A. Segura-Carretero, and A. Martínez-Férez. 2018. Development and Stability Evaluation of Water-in-edible Oils Emulsions Formulated with the Incorporation of Hydrophilic Hibiscus Sabdariffa Extract. *Food chemistry*. 260: 200–207.
[15] Y. Singh *et al.* 2017. Nanoemulsion: Concepts, Development and Applications in Drug Delivery. *Journal of Controlled Release*. 252: 28–49.
[16] S. Noori, F. Zeynali, and H. Almasi. 2018. Antimicrobial and Antioxidant Efficiency of Nanoemulsion-based Edible Coating Containing Ginger (*Zingiber officinale*) Essential Oil and Its Effect on Safety and Quality Attributes of Chicken Breast Fillets. *Food Control*. 84: 312–320.
[17] M. N. Yukuyama *et al.* 2019. Olive Oil Nanoemulsion Preparation using High-pressure Homogenization and d-phase Emulsification – A Design Space Approach. *Journal of Drug Delivery Science and Technology*. 49: 622–631.
[18] G. Gallego, M. Hakkarainen, and M. P. Almajano. 2017. Stability of O/W Emulsions Packed with PLA Film with Incorporated Rosemary and Thyme. *European Food Research and Technology*. 243(7): 1249–1259.
[19] L.-C. Peng, C.-H. Liu, C.-C. Kwan, and K.-F. Huang. 2010. Optimization of Water-in-oil Nanoemulsions by Mixed Surfactants. *Colloids and Surfaces A: Physicochemical and Engineering Aspects*. 370(1): 136-142.
[20] C.-X. Liang, D.-L. Qi, L.-N. Zhang, P. Lu, and Z.-D. Liu. 2021. Preparation and Evaluation of a Water-in-oil Nanoemulsion Drug Delivery System Loaded with Salidroside. *Chinese Journal of Natural Medicines*. 19(3): 231–240.
[21] K. O. Aboalnaja, S. Yaghmoor, T. A. Kumosani, and D. J. McClements. 2016. Utilization of Nanoemulsions to Enhance Bioactivity of Pharmaceuticals, Supplements, and Nutraceuticals: Nanoemulsion Delivery Systems and Nanoemulsion Excipient Systems. *Expert Opinion on Drug Delivery*. 13(9): 1327-1336.
[22] I. Y. Sudi, M. U. Ahmed, and B. Adzu. 2021. Sphaeranthus Senegalensis DC: Evaluation of Chemical Constituents, Oral Safety, Gastroprotective Activity, and Mechanism of Action of Its Hydroethanolic Extract. *Journal of Ethnopharmacology*. 268: 113597.
[23] C. A. Rabelo, N. Taarji, N. Khalid, I. Kobayashi, M. Nakajima, and M. A. Neves. 2018. Formulation and Characterization of Water-in-oil Nanoemulsions Loaded with Acai Berry Anthocyanins: Insights of Degradation Kinetics and Stability Evaluation of Anthocyanins and Nanoemulsions. *Food Research International*. 106: 542–548.
[24] M. Rafi *et al.* 2018. Total Phenolics, Flavonoids, and Anthocyanin Contents of Six Vireya Rhododendron from Indonesia and Evaluation of Their Antioxidant Activities. *Journal of Applied Pharmaceutical Science*. 8(09): 049–054.
[25] J. P. Maran, V. Sivakumar, K. Thirugnanasambandham, and R. Sridhar. 2015.Extraction of Natural Anthocyanin and Colors from Pulp of Jamun Fruit. *Journal of Food Science and Technology*. 52(6): 3617–3626.
[26] N. Wang and X. W. Yang. 2010. Two New Flavonoid Glycosides from the Whole Herbs of Hyssopus Officinalis. *J. Asian Nat. Prod. Res.* 12: 1044.
[27] R. Raviadaran, M. H. Ng, S. Manickam, and D. Chandran. 2019. Ultrasound-assisted Water-in-palm Oil Nano-emulsion: Influence of Polyglycerol Polyricinoleate and NaCl on Its Stability. *Ultrasonics sonochemistry*. 52: 353–363.
[28] H. Sun *et al.* 2023. Stabilization of Flaxseed Oil Nanoemulsions based on Flaxseed Gum: Effects of Temperature, pH and NaCl on Stability. *LWT*. 176: 114512.
[29] M. Tabibiazar and H. Hamishehkar. 2015. Formulation of a Food Grade Water-in-oil Nanoemulsion: Factors Affecting on Stability. *Pharmaceutical Sciences*. 21(4): 220–224.
[30] S. Samson, M. Basri, H. R. F. Masoumi, R. A. Karjiban, and E. A. Malek. 2016. Design and Development of a Nanoemulsion System Containing Copper Peptide by D-optimal Mixture Design and Evaluation of Its Physicochemical Properties. *RSC Advances*. 6(22): 17845–17856.
[31] S. Samson, M. Basri, H. R. Fard Masoumi, E. Abdul Malek, and R. Abedi Karjiban. 2016. An Artificial Neural Network based Analysis of Factors Controlling Particle Size in a Virgin Coconut Oil-based Nanoemulsion System Containing Copper Peptide. *PloS one*. 11(7): e0157737.
[32] L. Pavoni, D. R. Perinelli, G. Bonacucina, M. Cespi, and G. F. Palmieri. 2020. An Overview of Micro-and Nanoemulsions as Vehicles For Essential Oils: Formulation, Preparation Aand Stability. *Nanomaterials*. 10(1): 135.
[33] A.-M. Hafedh, W. A. H. Altowayti, and S. P. M. Bohari. 2020. In Vitro Study of Antidiabetic Effect of Abrus Precatorius Methanol Leaves Extract against Glucose Absorption," *International Journal of Life Sciences and Biotechnology*. 3(2): 117–126.
[34] P. Saini and M. Gangwar. 2017. Enzyme and Free Radical Inhibitory Potentials of Ethyl Acetate Extract of Endophytic Actinomycete from Syzygium Cumini.
[35] W. Zhang *et al.* 2010. Synthesis and Characterization of Thermally Responsive Pluronic F127−chitosan Nanocapsules for Controlled Release and Intracellular Delivery of Small Molecules. *ACS Nano*. 4(11): 6747–6759.
[36] S. K. Basha and V. S. Kumari. 2012. In Vitro Antidiabetic Activity of Psidium Guajava Leaves Extracts. *Asian Pacific Journal of Tropical Disease*. 2: S98–S100.
[37] A. Escobar-Ortiz, E. Castaño-Tostado, N. E. Rocha-Guzmán, J. A. Gallegos-Infante, and R. Reynoso-Camacho. 2021. Anthocyanins Extraction from *Hibiscus sabdariffa* and Identification of Phenolic Compounds Associated with Their Stability. *Journal of the Science of Food and Agriculture*. 101(1): 110–119.
[38] G. I. Peredo Pozos *et al.* 2020. Antioxidant Capacity and Antigenotoxic Effect of *Hibiscus sabdariffa L.* Extracts Obtained with Ultrasound-qssisted Extraction Process. *Applied Sciences*. 10(2): 560.
[39] B. R. Albuquerque, S. A. Heleno, M. B. P. Oliveira, L. Barros, and I. C. Ferreira. 2021. Phenolic Compounds: Current Industrial Applications, Limitations and Future Challenges. *Food & Function*. 12(1): 14–29.
[40] W. Ahmed *et al.* 2021. The Analysis of New Higher Operative Bioactive Compounds and Chemical Functional Group from Herbal Plants through UF-HPLC-DAD and Fourier Transform Infrared Spectroscopy Methods and Their Biological Activity with Antioxidant Potential Process as Future Green Chemical Assay. *Arabian Journal of Chemistry*. 14(2): 102935.
[41] I. Borrás-Linares *et al.* 2015. Characterization of Phenolic Compounds, Anthocyanidin, Antioxidant and Antimicrobial Activity of 25 Varieties of Mexican Roselle (Hibiscus sabdariffa). *Industrial Crops and Products*. 69: 385–394.
[42] Z. S. Ahmed and S. S. Abozed. 2015. Functional and Antioxidant Properties of Novel Snack Crackers Incorporated with Hibiscus sabdariffa by-product. *Journal of Advanced Research*. 6(1): 79–87.
[43] S. Sukkhaeng, S. Promdang, and U. Doung-ngern. 2018. Fruit Characters and Physico-chemical Properties of Roselle (Hibiscus sabdariffa L.) in Thailand—A Screening of 13 New

Genotypes. *Journal of Applied Research on Medicinal and Aromatic Plants*. 11: 47–53.
[44] A. R. Mansur, J. Oh, H. S. Lee, and S. Y. Oh. 2021. Determination of Ethanol in Foods and Beverages by Magnetic Stirring-assisted Aqueous Extraction Coupled with GC-FID: A Validated Method for Halal Verification. *Food Chemistry*. 366: 130526.
[45] N. Pauzi, S. Man, M. S. A. M. Nawawi, and M. F. Abu-Hussin. 2019. Ethanol Standard in Halal Dietary Product among Southeast Asian Halal Governing Bodies. *Trends in Food Science & Technology*. 86: 375–380.
[46] N. B. Romes, R. A. Wahab, M. Abdul Hamid, and S. E. Hashim. 2020. D-optimal Design-assisted Elaeis Guineensis Leaves Extract in Olive Oil-sunflower Seed Nanoemulsions: Development, Characterization, and Physical Stability. *Journal of Dispersion Science and Technology*. 1–13.
[47] N. H. Che Marzuki, R. A. Wahab, and M. Abdul Hamid. 2019. An Overview of Nanoemulsion: Concepts of Development and Cosmeceutical Applications. *Biotechnology & Biotechnological Equipment*. 33(1): 779–797.
[48] A. O. Baba Shekh, R. Abdul Wahab, and N. A. Yahya. 2022. Formulation of Roselle Extract Water-in-oil Nanoemulsion for Controlled Pulmonary Delivery. *Journal of Dispersion Science and Technology*. 1–12.
[49] M. Danaei *et al.* 2018. Impact of Particle Size and Polydispersity Index on the Clinical Applications of Lipidic Nanocarrier Systems. *Pharmaceutics*. 10(2): 57.
[50] A. M. Cheong, C. P. Tan, and K. L. Nyam. 2016. In Vitro Evaluation of the Structural and Bioaccessibility of Kenaf Seed Oil Nanoemulsions Stabilised by Binary Emulsifiers and B-Cyclodextrin Complexes. *Journal of Food Engineering*. 189: 90–98.
[51] S. Mohamadi Saani, J. Abdolalizadeh, and S. Zeinali Heris. 2019. Ultrasonic/sonochemical Synthesis and Evaluation of Nanostructured Oil in Water Emulsions for Topical Delivery of Protein Drugs. *Ultrasonics Sonochemistry*. 55: 86–95.
[52] M. M. H. Shah Buddin, A. L. Ahmad, A. T. Abd Khalil, and S. W. Puasa. 2020. A Review of Demulsification Technique and Mechanism for Emulsion Liquid Membrane Applications. *Journal of Dispersion Science and Technology*. 1–18.
[53] J. B. Aswathanarayan and R. R. Vittal. 2019. Nanoemulsions and Their Potential Applications in Food Industry. *Frontiers in Sustainable Food Systems*. 3: 95.
[54] S.-H. Kuo, C.-J. Shen, C.-F. Shen, and C.-M. Cheng. 2020. Role of pH value in Clinically Relevant Diagnosis. *Diagnostics*. 10(2): 107.
[55] H.-Y. Son *et al.* 2019. Formulation and Characterization of Quercetin-loaded Oil in Water Nanoemulsion and Evaluation of Hypocholesterolemic Activity in Rats. *Nutrients*. 11(2): 244.
[56] N. F. Dzulkifli, A. Mamat, and I. A. Choudhury. 2020. The Potential of Water-In-Oil Emulsion of Canola Oil as Dielectric Fluid for EDM Process. *Journal of Advanced Research in Fluid Mechanics and Thermal Sciences*. 72(2): 129–141.
[57] Y. Q. Almajidi, Z. H. Mahdi, and N. K. Maraie. 2018. Preparation and in Vitro Evaluation of Montelukast Sodium Oral Nanoemulsion. *Int J Appl Pharm*. 10: 49–53.
[58] Y. Wang and T. H. Hahn. 2007. AFM Characterization of the Interfacial Properties of Carbon Fiber Reinforced Polymer Composites Subjected to Hygrothermal Treatments. *Composites Science and Technology*. 67(1): 92–101.
[59] N. B. Romes, R. Abdul Wahab, M. Abdul Hamid, H. A. Oyewusi, N. Huda, and R. Kobun. 2021. Thermodynamic Stability, In-vitro Permeability, and In-silico Molecular Modeling of the Optimal Elaeis Guineensis Leaves Extract Water-in-oil Nanoemulsion. *Scientific Reports*. 11(1): 1–19.
[60] V. V. Changediya, R. Jani, and P. Kakde. 2019. A Review on Nanoemulsions: A Recent Drug Delivery Tool. *Journal of Drug Delivery and Therapeutics*. 9(5): 185–191.
[61] H. E. Khoo, A. Azlan, S. T. Tang, and S. M. Lim. 2017. Anthocyanidins and Anthocyanins: Colored Pigments as Food, Pharmaceutical Ingredients, and the Potential Health Benefits. *Food & Nutrition Research*. 61(1): 1361779.
[62] S. N. A. Syed Azhar, S. E. Ashari, and N. Salim. 2018. Development of a Kojic Monooleate-enriched oil-in-water Nanoemulsion as a Potential Carrier for Hyperpigmentation Treatment. *International Journal of Nanomedicine*. 6465–6479.
[63] P. Karthik, P. Ezhilarasi, and C. Anandharamakrishnan. 2017. Challenges Associated in Stability of Food Grade Nanoemulsions. *Critical Reviews in Food Science and Nutrition*. 57(7): 1435–1450.
[64] S. Neumann, U. S. van der Schaaf, and H. Schuchmann. 2017. The Diffusion and Coalescence Time Analyzer (DCTA): A Novel Experimental Setup for Investigating Instability Phenomena in Double Emulsions. *Food Structure*. 12: 103–112.
[65] M. G. P. Malode, S. A. Chauhan, S. A. Bartare, L. M. Malode, J. V. Manwar, and R. L. Bakal. 2022. A Critical Review on Nanoemulsion: Advantages, Techniques and Characterization. *Journal of Applied Pharmaceutical Sciences and Research*. 4(3): 6–12.
[66] J. Adiotomre, M. A. Eastwood, C. Edwards, and W. G. Brydon. 1990. Dietary Fiber: In Vitro Methods that Anticipate Nutrition and Metabolic Activity In Humans. *The American Journal of Clinical Nutrition*. 52(1): 128–134.
[67] C. Palanuvej, S. Hokputsa, T. Tunsaringkarn, and N. Ruangrungsi. 2009. In Vitro Glucose Entrapment and Alpha-glucosidase Inhibition of Mucilaginous Substances from Selected Thai Medicinal Plants. *Scientia Pharmaceutica*. 77(4): 837–850.
[68] S. Senapati, A. K. Mahanta, S. Kumar, and P. Maiti. 2018. Controlled Drug Delivery Vehicles for Cancer Treatment and Their Performance. *Signal Transduction and Targeted Therapy*. 3(1): 1–19.
[69] A. S. Patel, S. Lakshmibalasubramaniam, and B. Nayak. 2020. Steric Stabilization of Phycobiliprotein Loaded Liposome through Polyethylene Glycol Adsorbed Cellulose Nanocrystals and Their Impact on the Gastrointestinal Tract. *Food Hydrocolloids*. 98: 105252.